Fırat Üniversitesi Deneysel ve Hesaplamalı Mühendislik Dergisi

FUJECE

Hidrotermal Karbonizasyon Yöntemiyle Biyokütle Bazlı Aktif Karbon Üretim Prosesinin Geliştirilmesi

Nida KATI[1], Ferhat UÇAR[2*]

[1]Metalurji ve Malzeme Mühendisliği, Teknoloji Fakültesi, Fırat Üniversitesi, Elazığ, Türkiye.
[2]Yazılım Mühendisliği, Teknoloji Fakültesi, Fırat Üniversitesi, Elazığ, Türkiye.
[1]nkati@firat.edu.tr, [2]fucar@firat.edu.tr

Geliş Tarihi: 26.04.2024
Kabul Tarihi: 07.06.2024
Düzeltme Tarihi: 21.05.2024
doi: 10.62520/fujece.1473852
Araştırma Makalesi

Alıntı: N. Katı ve F. Uçar, "Hidrotermal karbonizasyon yöntemiyle biyokütle bazlı aktif karbon üretim prosesinin geliştirilmesi", Fırat Üni. Deny. ve Hes. Müh. Derg., vol. 3, no 3, pp. 326-336, Ekim 2024.

Öz

Bu çalışma, kayısı çekirdeği kabukları (KÇK) kullanılarak hidrotermal karbonizasyon ve kimyasal aktivasyon yöntemleriyle üretilen hidrokömürlerin ve aktif karbonların ayrıntılı karakterizasyonunu içeren bir süreç geliştirmeyi sunmaktadır. İlk olarak, KÇK öğütülerek işlenmiş, ardından 24, 36 ve 48 saat boyunca 240ºC'de hidrotermal karbonizasyona tabi tutularak üç farklı hidrokömür elde edilmiştir. Daha sonra, bu hidrokarbonlar 3 saat boyunca KOH ile karıştırılmış ve aktif karbonlar elde etmek için 700°C'de 1 saat boyunca karbonizasyon işlemine tabi tutulmuştur. Aktif karbonların yapısal özelliklerini belirlemek için Brunauer-Emmett-Teller (BET) yüzey alanı analizi, Taramalı Elektron Mikroskobu (SEM) ve Enerji Dağılım Spektroskopisi (EDS), X-Işını Kırınımı (XRD) analizi ve Fourier-Transform Kızılötesi spektroskopisi (FTIR) ölçümleri gibi çeşitli karakterizasyon yöntemleri kullanılmıştır. Elde edilen sonuçlar, hidrotermal reaksiyon süresinin karbon içeriğini artırdığını ve gözenekli yapıların oluşumuna yol açtığını göstermektedir. Özellikle, SEM görüntülerinden de anlaşılacağı üzere, kimyasal aktivasyon sürecinin gözenek oluşumunda etkili olduğu görülmüştür. Sonuç olarak, bu çalışma hidrokömürlerin ve KÇK'den elde edilen aktif karbonların karakteristik özelliklerinin ayrıntılı bir tanımını sunmaktadır.

Anahtar kelimeler: Hidrotermal karbonizasyon, Aktif karbon, Kayısı çekirdeği kabuğu

*Yazışılan Yazar

İntihal Kontrol: Evet – Turnitin
Şikayet: fujece@firat.edu.tr

Firat University Journal of Experimental and Computational Engineering

Development of a Production Process for Biomass-Based Activated Carbon via Hydrothermal Carbonization Method

Nida KATI[1], Ferhat UÇAR[2*]

[1]Metalurgical and Materials Engineering, Faculty of Technology, Fırat University, Elazığ, Türkiye.
[2]Software Engineering, Faculty of Technology, Fırat University, Elazığ, Türkiye.
[1]nkati@firat.edu.tr, [2]fucar@firat.edu.tr

Received: 26.04.2024
Accepted: 07.06.2024
Revision: 21.05.2024
doi: 10.62520/fujece.1473852
Research Article

Citation: N. Katı and F. Uçar, "Development of a Production Process for Biomass-Based Activated Carbon via Hydrothermal Carbonization Method", Firat Univ. Jour.of Exper. and Comp. Eng., vol. 3, no 3, pp. 326-336, October 2024.

Abstract

This study presents a process development including detailed characterization of hydrochars and activated carbons produced by hydrothermal carbonization and chemical activation methods using apricot kernel shells (AKS). Initially, the AKS were processed by grinding, followed by subjecting them to hydrothermal carbonization at 240ºC for 24, 36, and 48 hours, resulting in three distinct hydrochars. Subsequently, these hydrochars were mixed with KOH for 3 hours and subjected to a carbonization process at 700°C for 1 hour to obtain activated carbons. Various characterization methods such as Brunauer-Emmett-Teller (BET) surface area analysis, Scanning Electron Microscopy (SEM) and Energy Dispersive Spectroscopy (EDS), X-Ray Diffraction (XRD) analysis, and Fourier-Transform Infrared spectroscopy (FTIR) measurements were employed to determine the properties of the activated carbons. The results obtained indicate that the duration of the hydrothermal reaction increases the carbon content and leads to the formation of porous structures. Particularly, the chemical activation process was found to be effective in pore formation, as evident in SEM images. In conclusion, this study provides a detailed description of the characteristic properties of hydrochars, and activated carbons derived from AKS.

Keywords: Hydrothermal carbonization, Activated carbon, Apricot kernel shell

*Corresponding Author

Plagiarism Checks: Yes – Turnitin
Complaints: fujece@firat.edu.tr

1. Introduction

Türkiye is the largest producer of fresh and dried apricots in the world. Consequently, a substantial amount of cheap apricot kernel shells (AKS), obtained as waste in apricot production, is available. Approximately 25,000 tons of AKS are generated annually in Türkiye as industrial waste. Through the utilization of activation techniques, around 4,000 tons of high value activated carbon can be produced from this biomass [1]. In 2021, Malatya accounted for 48.7% of the total apricot production in Türkiye with 389,000 tons of fresh apricots. Following Malatya, Mersin contributed 20.3%, Igdir .4%, Elazığ 3.9%, and Isparta 2.8% to the overall production [2]. Analysis of the AKS data used in our study indicates an annual yield of approximately 20,000 tons in the Malatya region [3]. Biomass structures can be converted into high-value components containing solid, liquid, and gaseous products using the hydrothermal method. The variation in specific properties depending on the temperature and pressure of water brings significant advantages to the processing of biomass with the hydrothermal method. During hydrothermal conversion, hot water, acting both as a solvent and as a reactive or catalytic agent, plays a crucial role. For instance, many cellulose-based biomasses are insoluble in water, but they can become soluble in supercritical water during the hydrothermal process. Additionally, another advantage of the hydrothermal method is its suitability as a thermochemical conversion method for biomass with high moisture content [4]. There are several studies in the literature regarding biomass waste, particularly AKS. L. Wang et al. synthesized activated carbon from apricot shell extract using chemical methods with the support of H_3PO_4 in a process, investigating the relationship between pore structure and electrochemical performance for supercapacitor applications [5]. In another proposed study by the same research group, activated carbon was produced from apricot shells using a one-step chemical synthesis method, and its supercapacitor performance was evaluated. The positive attributes contributed by the hierarchical pore structure in this study were presented in detail. The morphological structure of the activated carbon synthesized from AKS was demonstrated to provide a broad adsorption area, with micro-pores addressing the flow of electrolyte ions and storage capacity, and meso-pores and macro-pores serving as transport channels and buffer reservoirs for electrolyte ions, respectively [6]. Temirgaliyeva et al. prepared an active carbon and carbon nanotube-based composite material from three different biomass types, including AKS, proposing an electrode structure for use in hybrid supercapacitor [7]. Eom et al. analyzed the use of activated porous carbon obtained from spent black tea residues as long-lasting supercapacitor electrodes, emphasizing the suitability of its recyclable use [8]. Canbaz obtained active carbon electrodes through hydrothermal carbonization from hazelnut shell-derived biomass material and investigated their potential use for sodium-ion batteries [9].

This study pioneers a novel approach to the sustainable valorization of industrial biomass waste, specifically AKS, by utilizing the hydrothermal method to produce high value activated carbon especially for supercapacitor applications. **Our research stands out for its innovative contributions, which include:**

1. Innovative hydrothermal conversion process: We developed and optimized a unique hydrothermal conversion technique specifically designed for AKS. This method not only enhances the efficiency of biomass conversion but also improves the quality and functionality of the resulting activated carbon. Our process is distinguished by its ability to handle the high moisture content of biomass, which typically complicates biomass conversion efforts.

2. Detailed characterization and application of activated carbon: Our research provides an exhaustive characterization of the activated carbon produced, detailing its morphological properties. This contribution is significant as it bridges the gap between theoretical research and practical, commercial applications of activated carbons in supercapacitor technology.

These contributions not only advance the field of biomass waste management but also highlight the potential of agricultural waste to be transformed into economically valuable products, aligning with global sustainability goals and advancing green technology initiatives.

2. Material and Method

The AKS used as raw material in our study were obtained from the Elazig. The shells were ground to 60 mesh sizes using a laboratory-type blender (Waring blender), and the resulting powdered shells were stored in a glass jar. The Potassium Hydroxide (KOH) with CAS number 1310-58-3 used in the activation process and Hydrochloric Acid (HCl) from the Biorad brand used in the washing process were commercially obtained. The raw material, AKS powder (N-Raw), utilized as biomass for the preparation of hydrochars through hydrothermal carbonization, was mixed with 40 mL of distilled water to achieve a ratio of 4 grams in a stainless-steel reactor (Fytronix FYHT-8000 model) equipped with a Teflon vessel. The hydrothermal apparatus, manufactured by Fytronix Electronics, comprises a temperature and time-controlled control panel and a hydrothermal reactor. The inner part of the stainless-steel reactor is designed to accommodate a 100 ml Teflon vessel. The reactor's lid features two valves and a digital pressure gauge to facilitate gas inlet and outlet. After placing the mixture in the Teflon vessel, hydrochars were produced under hydrothermal carbonization conditions at 240°C for 24, 36, and 48 hours, resulting in hydrochars produced under three different parameters. The obtained hydrochars were filtered using membrane filter paper, washed with distilled water, and dried in an oven at 100°C for 24 hours. One-third of the dried products were separated, stored in a glass sample dish, and labeled as N-H1, N-H2, and N-H3. The remaining products were impregnated with commercially obtained KOH in a 1:3 ratio at a temperature between 60-70°C for 3 hours for chemical activation. The KOH-loaded hydrochars were filtered, dried in an oven at 100°C for 24 hours, transferred to a ceramic crucible, and subjected to carbonization in a tube furnace at 700°C for 1 hour with a nitrogen flow rate of 300 cm^3/min. The resulting activated carbons were then washed with HCl acid until reaching a pH of 6-7, followed by washing with distilled water and filtration. The filtered products were dried at 100°C for 24 hours. The obtained activated carbons were named N-A1, N-A2, and N-A3. Table 1 provides information on the samples and production parameters, while Figure 1 illustrates the production stages of the activated carbons.

Table 1. Samples and production parameters.

Sample Name	Hydrothermal Reaction Temperature (°C)	Hydrothermal Reaction Pressure (MPa)	Hydrothermal Reaction Time (hr)	Chemical Activation
N-H1	240	5-6	24	No Chemical Activation
N-H2	240	5-6	36	
N-H3	240	5-6	48	
N-A1	240	5-6	24	KOH
N-A2	240	5-6	36	
N-A3	240	5-6	48	

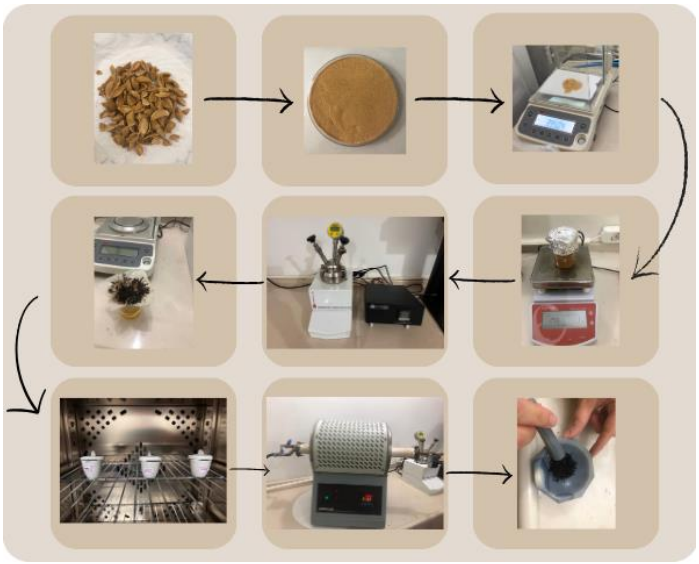

Figure 1. Activated carbon production stages.

To determine the surface area and pore size distribution of hydrochars and activated carbons, nitrogen adsorption was performed at -196°C using the Micromeritics ASAP 2020 instrument in the Department of Chemical Engineering at Fırat University. The hydrochars and activated carbons were subjected to vacuum treatment at 150°C for 12 hours, and nitrogen adsorption/desorption isotherms were obtained in the relative pressure (P/P_0) range of 0-1. The surface area (SBET) of the adsorbents was determined using the Brunauer-Emmet-Teller (BET) method based on nitrogen adsorption/desorption isotherm data. For the structural characterization of untreated AKS, hydrochars, and activated carbons, Scanning Electron Microscopy (SEM) and Energy Dispersive Spectroscopy (EDS) analysis was conducted using the JEOL JSM-7001F model SEM instrument available at the KITAM Laboratory of Ondokuz Mayıs University. X-Ray Diffraction (XRD) analyses of the samples were carried out using the SmartLab X-RAY Diffractometer XRD instrument at the KITAM Laboratory of Ondokuz Mayıs University. XRD measurements were performed in the $2\theta = 20° - 80°$ angle range with values of 45 kV and 40 mA. To identify the functional bonds in the molecular structure of the samples, Fourier-Transform Infrared spectroscopy (FTIR) measurements were conducted using the Thermo SCIENTIFIC Nicolet iS5 Spectrophotometer apparatus in the Central Laboratory of Fırat University (spectrum range 4000-400 cm^{-1}).

3. Results and Discussion

BET surface area values of hydrochar and activated carbons produced by the hydrothermal carbonization method are given in Table 2. When examining the BET surface area values of hydrochars produced through hydrothermal reaction, it can be stated that the reaction duration has an impact on the surface area. Comparing the raw AKS sample (N-Raw) with the processed samples N-H1 to N-H3, the hydrothermal process increased the bet surface area. As the particle size of the material decreases, an increase in surface area occurs. The presence of a porous structure, as evident in the SEM images in Figure 2, supports this increase. The lower porosity of samples obtained through the hydrothermal carbonization of biomass explains their lower surface areas [10]. The BET surface areas of samples obtained from lignocellulosic biomass generally show similarities with the literature. The application of KOH activation to hydrochars results in an increase in surface areas [11], [12], [13]. The highest surface area value, 976.650 m^2/g, was found in the N-A3 sample subjected to a 48-hour hydrothermal reaction and KOH activation. The activating agent plays a significant role in the development of the porous structure. In another study in the literature, samples obtained through hydrothermal carbonization at 280°C for 1 hour, 3 hours, and 6 hours showed an increase in BET surface area values from 46 m^2/g to 92 m^2/g with increasing reaction time. It was indicated that the trend of increased surface areas with extended reaction time is related to the surface roughness resulting from the transformation of cellulose, hemicellulose, and lignin present in lignocellulosic biomass [14], [15].

Table 2. BET surface area results of the samples

Sample Name	BET surface area (m^2/g)
N-Raw	4.2756
N-H1	5.8682
N-H2	20.7856
N-H3	80.6333
N-A1	637.970
N-A2	842.310
N-A3	976.650

SEM analysis was performed to evaluate the surface structures of AKS powder (N-Raw) without hydrothermal carbonization, hydrochar obtained by hydrothermal carbonization, and activated carbon samples with the activation process. SEM images provide important information about the physical morphology of the surface. The changes occurring on the surface and the micro and mesopores formed before and after the hydrothermal carbonization process applied to the raw apricot seed shell and after the carbonization process can be seen in the SEM images.

The SEM images of raw apricot kernel shell (N-Raw), samples subjected to hydrothermal reactions at 240 °C for 24 hours, 36 hours, and 48 hours (N-H1, N-H2, and N-H3), and activated carbons named N-A1, N-A2, and N-A3 after carbonization are presented in Figure 2.

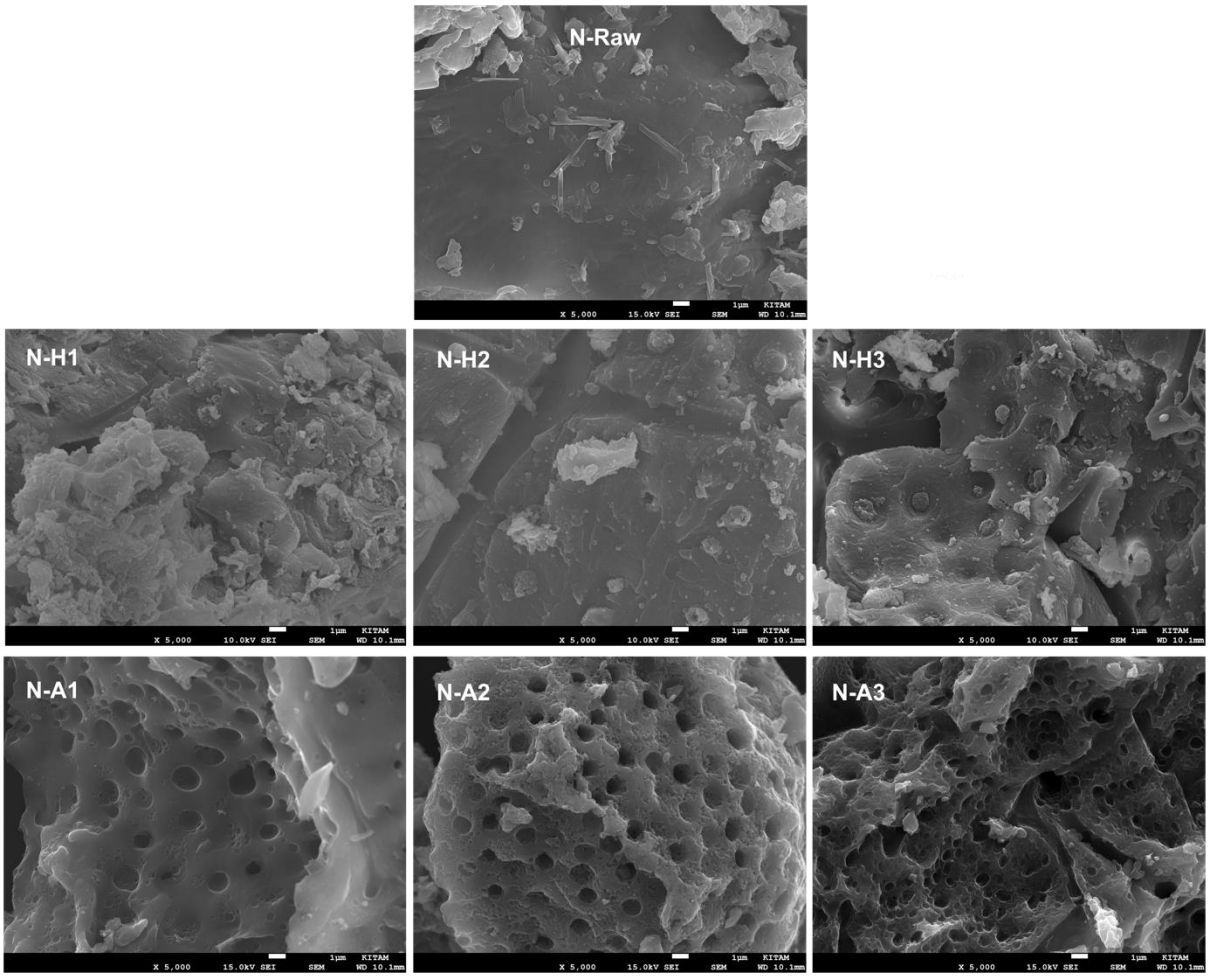

Figure 2. SEM images (5000x) of N-Raw, N-H1, N-H2, N-H3, N-A1, N-A2 and N-A3 samples

Upon examination of the SEM images of the N-Raw sample and the samples obtained after hydrothermal reaction, it is observed that N-H1 and N-H2 samples do not exhibit a porous structure, and the surface is smooth. However, a porous structure is observed in the N-H3 sample. When SEM images of activated carbons subjected to carbonization (N-A1, N-A2, and N-A3) are examined, porous structures are observed. In all samples, the pore structures are irregular and form a block-like void structure. The surfaces are uneven with protrusions and recesses. SEM images indicate that the chemical activation process applied after the hydrothermal reaction is effective in pore formation. KOH, as an activation agent, facilitated the faster degradation of the raw material structure during the carbonization process. During carbonization, the product's structure was significantly degraded through thermal decomposition, and many functional groups were removed from the structure.

As volatile substances were largely removed, a porous structure was obtained. Consistent with the literature findings, SEM images suggest that the activation method applied with KOH is effective in pore formation [16]. In another study in the literature, AKS, after chemical activation, exhibited pores mostly in the interparticle areas, and the surface was disrupted with strong $ZnCl_2$ activation, resulting in the formation of pores and cell configuration [17]. From the SEM images, it is evident that the hydrothermal carbonization method significantly affected the surface of the N-Raw sample. The obtained activated carbons clearly show pores formed on the surface in SEM images. The breaking of bonds in the raw material's structure and the separation of volatile compounds from the structure due to the influence of temperature and pressure result in the formation of pores, cracks, and cavities on the surface. The decomposition of hemicellulose, which is more easily broken down compared to cellulose, and the formation of a rough and even porous surface may

lead to increased surface roughness depending on the reaction temperature in reactions taking place in aqueous environments [18].

Conducting the EDS analyses, EDS maps of the N-H3 sample subjected to 240 °C for 48 hours of hydrothermal reaction to observe the effect of reaction time on the structure and the N-A3 sample subjected to activation with KOH are presented in Figures 3 and 4, respectively.

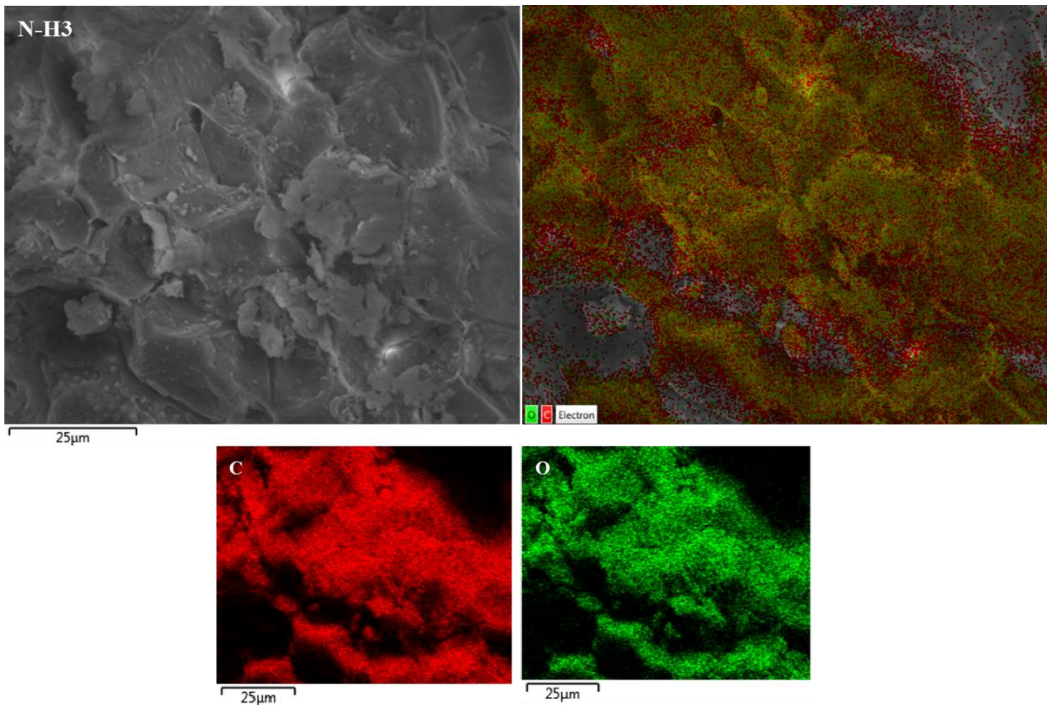

Figure 3. Elemental map of the N-H3 sample

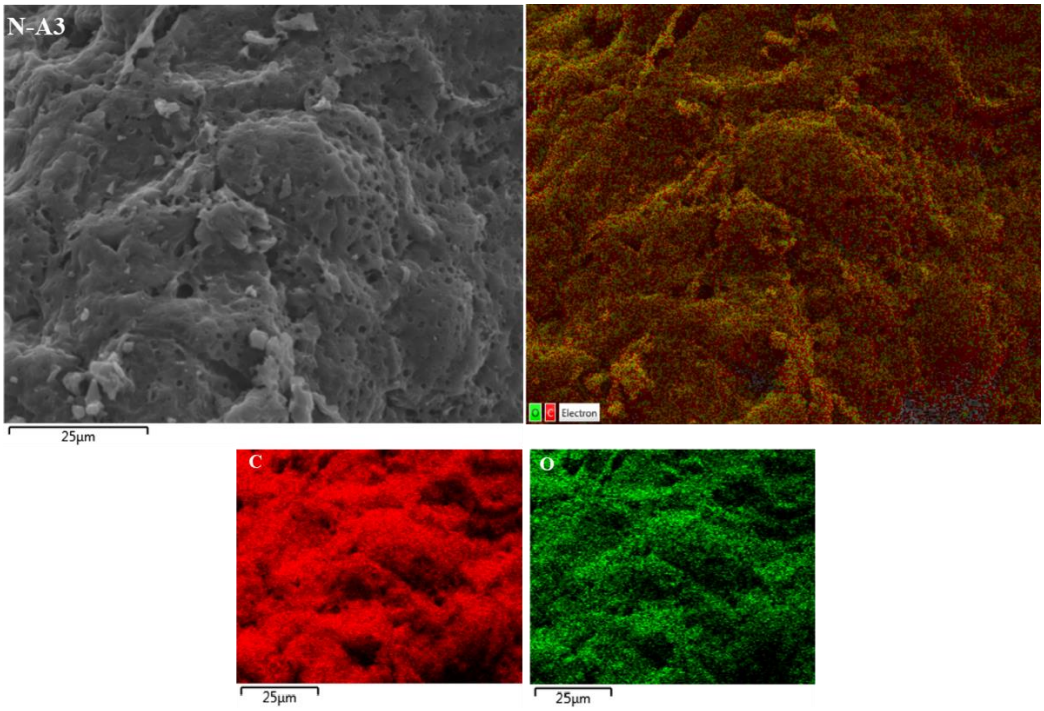

Figure 4. Elemental map of the N-A3 sample

Elemental analysis results for all samples are provided in Table 3. It is observed that as the hydrothermal reaction time increases, the carbon content increases and the oxygen content decreases in all samples obtained as a result of the hydrothermal reaction and carbonization process. During hydrothermal carbonization, organic materials transform into carbon, a process known as carbonization. This carbonization process can lead to an increase in carbon ratios as organic components turn into carbon. The increase in carbon content after the activation process is a result of the conversion of organic compounds into carbon. Under high temperature and pressure, hydrothermal conditions cause oxygen to react with water. In this case, oxygen molecules can combine with water to form volatile gases or other forms that can exit the system. This can result in a decrease in oxygen ratios. Additionally, chemical transformations of organic materials during hydrothermal carbonization can break the bonds between oxygen and organic components, leading to a decrease in oxygen ratios in these chemical transformations. Hydrothermal carbonization processes carried out at different durations can yield different results depending on the process duration. Longer processes result in increased carbonization and the removal of oxygen from the system.

Table 3. The weight-based elemental ratios of the samples

Sample	Weight Ratios of Elements (%)					
	C	O	Mg	K	Ca	S
N-Raw	59.83	36.66	0.18	1.55	0.69	1.09
N-H1	68.98	31.02	-	-	-	-
N-H2	69.13	30.87	-	-	-	-
N-H3	69.31	30.69	-	-	-	-
N-A1	83.44	16.01	0.31	-	0.24	-
N-A2	84.02	15.63	0.10	-	-	-
N-A3	88.14	11.86	-	-	-	-

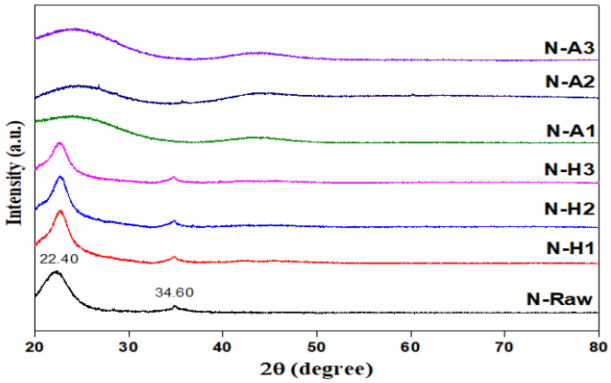

Figure 5. The XRD spectra of the samples

X-ray diffraction analyses were conducted to determine the changes in the crystal structure of AKS, hydrochars, and activated carbons. In Figure 5, X-ray diffraction patterns for these samples are presented. In the raw AKS biomass, two peaks are observed at 2θ=22.40° and 2θ=34.60°. The XRD peak at 2θ=22.40° is characteristic of amorphous carbon, while the second, smaller peak around 2θ=34.60° can be attributed to the typical cellulose I structure, specifically to the (004) lattice plane. The presence of free hydroxyl groups, allowing for a regular crystal arrangement in cellulose, leads to intra- and intermolecular hydrogen bonding [19]. The structure of hydrochars obtained through hydrothermal reaction was found to be similar to the AKS sample, with the only difference being a slight broadening of the sharp peak. This broadening observed in the peaks after hydrothermal reaction at different durations indicates the initiation of structural degradation. Despite the carbon-based nature of our raw material, these broadened peaks suggest the onset of amorphous carbon formation. However, it is noted that the conditions of 240°C temperature and reaction durations of 24, 36, and 48 hours are insufficient for the complete elimination of cellulose's crystal structure. In samples activated with KOH at 700°C under an N_2 gas atmosphere, the peaks related to cellulose gradually broaden, indicating the formation of an amorphous structure. It is observed that the hydrothermal carbonization process induces chemical changes in the AKS powder, leading to the formation of an entirely different product.

The comparative FTIR spectra of raw AKS, hydrochars, and activated carbons are shown in Figure 6. The spectrum of the raw apricot kernel shell exhibits a broad band at 3722 cm^{-1}, attributed to the absorption of hydroxyl groups in polysaccharides [20], [21]. This result indicates that polysaccharides, including cellulose, hemicellulose, and lignin, are the main components of the apricot kernel shell. The bands at 3000–3600 cm^{-1} in raw AKS and hydrochar samples correspond to the O-H stretching vibrations of hydroxyl or carboxyl groups [22].

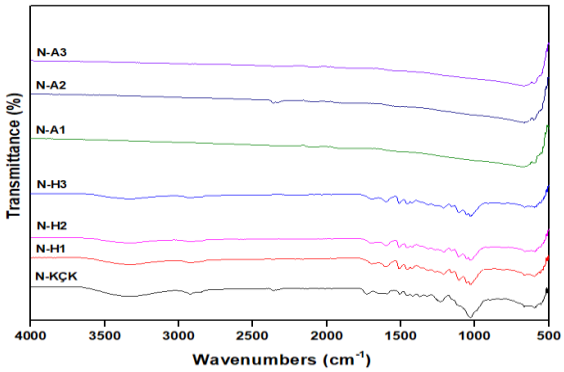

Figure 6. FTIR spectra of the samples

The two bands at 2923 and 2851 cm^{-1} in the raw AKS and hydrochar samples correspond to the asymmetric and symmetric stretching vibrations of methyl and methylene groups in cellulose, hemicellulose, and lignin [23]. The peak at 1734 cm^{-1} is attributed to the C=O stretching vibration of ester groups in hemicellulose and lignin [24]. The peak at 1026 cm^{-1} in the spectrum of raw AKS and hydrochar samples is related to the β-glycosidic bond in cellulose and hemicellulose [25, 26]. The strong C–O band at around 1100 cm^{-1} indicates the C–H aromatic plane bending from the $–OCH_3$ in the lignin structure, while the bending of the aromatic plane at approximately 833 cm^{-1} is observed. In hydrochar samples, a weak peak at 3455 cm^{-1} indicates -OH groups, possibly a result of phenolic-hydroxyl cleavage [19, 27]. After activation with KOH, some vibrations disappear, and some peaks shift. In the N-A2 sample, a C≡C stretching vibration of alkyne groups is observed at 2300 cm^{-1}, which is not present in other activated samples [28]. The peak at 1230 cm^{-1}, indicating the G (guaiacyl) unit in lignin, disappears after activation, suggesting the degradation of the lignin structure. The ester carbonyl groups at 1734 cm^{-1} in the spectrum of the raw sample are completely lost in the activated carbon samples due to decomposition at high operating temperatures [29]. The aromatic skeleton vibrations at 1585 and 1505 cm^{-1} observed in the spectrum of the raw sample, attributed to lignin, are completely absent in the activated carbon samples due to the transformation of phenyl chains [30, 31]. Additionally, the peak around 1026 cm^{-1} is almost absent in activated carbon samples, indicating the decomposition of hemicellulose and cellulose. The absence of a band at 1102 cm^{-1} in activated carbon samples also suggests the loss of $–OCH_3$ due to deoxygenation reactions [32, 33].

4. Conclusion

This study provides a detailed characterization of hydrochars and activated carbons produced through hydrothermal carbonization and chemical activation methods using AKS. Initially, AKS were ground and subjected to hydrothermal carbonization at 240°C for 24, 36, and 48 hours, resulting in three different hydrochars. Subsequently, these hydrochars were chemically activated with KOH, mixed for 3 hours, and carbonized at 700°C for 1 hour to obtain activated carbons. Various characterization methods, including BET surface area, SEM analysis, XRD analysis, and FTIR measurements, were employed to determine the properties of the activated carbons. The results indicated that the hydrothermal reaction duration increased carbon content and led to the formation of porous structures. Chemical activation with KOH further enhanced the surface area, particularly evident in SEM images. The study highlighted the effectiveness of the activation process in pore formation, as indicated by irregular pore structures observed in all activated carbon samples. SEM analysis was instrumental in evaluating the surface morphologies of raw AKS powder (N-Raw), hydrochars obtained through hydrothermal carbonization (N-H1, N-H2, and N-H3), and activated carbons (N-A1, N-A2, and N-A3). The images revealed a lack of porous structure in N-H1 and N-H2 samples, while a porous structure was observed in N-H3. Activated carbons displayed consistent irregular pore structures

with protrusions and recesses, emphasizing the effectiveness of the KOH activation process in pore formation. Elemental analysis results showed an increase in carbon content and a decrease in oxygen content with extended hydrothermal reaction time, indicating the transformation of organic materials into carbon. X-ray diffraction analyses revealed changes in the crystal structure, with hydrochars exhibiting amorphous carbon formation. Comparative FTIR spectra of raw AKS, hydrochars, and activated carbons demonstrated shifts and disappearances of peaks, reflecting chemical transformations during the hydrothermal carbonization and activation processes. The study concluded that hydrothermal carbonization and chemical activation significantly influenced the physical, surface, and chemical properties of hydrochars and activated carbons obtained from apricot kernel shells, showcasing their potential for diverse applications.

5. Acknowledgement

We gratefully acknowledge the support of The Scientific and Technological Research Council of Türkiye (TÜBİTAK), which has generously funded our research under Project Number 122M793. Also, some analyzes of the study have been conducted with the support of Fırat University Scientific Research Projects Coordination Unit (FÜBAP) under the Project Number ADEP 23.19.

6. Author Credit Statement

All authors contributed equally to this work in the conception of the idea, the design of the study, and conducting the literature review along with the acquisition of data, performing the analysis, and critically revising the manuscript for important intellectual content. Both authors collaborated closely in sourcing materials and resources needed for the study. Each author contributed significantly to the writing and editing of the manuscript, ensuring that the final version submitted for publication met all necessary criteria for accuracy and integrity.

7. Ethics Committee Approval and Conflict of Interest

"There is no conflict of interest with any person/institution in the prepared article"

8. References

[1] G. Hekimoğlu, A. Sarı, Y. Önal, O. Gencel, V. V. Tyagi, and E. Aslan, "Utilization of waste apricot kernel shell derived-activated carbon as carrier framework for effective shape-stabilization and thermal conductivity enhancement of organic phase change materials used for thermal energy storage," Powder Technol., vol. 401, p. 117291, Mar. 2022.
[2] T. Ekonomi and P. Geliştirme Enstitüsü, "Hazırlayan Mine Hasdemir."
[3] E. Haberleri, "Kabuk diye sakın çöpe atmayın! Bu ilimize yıllık 12 milyon kazandırıyor - Ekonomi Haberleri." Accessed: Nov. 09, 2023. [Online]. Available: https://www.sabah.com.tr/ekonomi/2019/01/01/kabuk-diye-sakin-cope-atmayin-bu-ilimize-yillik-12-milyon-kazandiriyor
[4] M. Ahtik, "Antep Fıstığı Kabuğundan Hidrotermal Karbon Üretimi ve Karakterizasyonu," Karabük Üniv., 2022, (In Turkish).
[5] L. Wang et al., "H3PO4-assisted synthesis of apricot shell lignin-based activated carbon for capacitors: Understanding the pore structure/electrochemical performance relationship," Ener. and Fuels, vol. 35, no. 9, pp. 8303–8312, May 2021.
[6] L. Wang, L. Xie, H. Wang, H. Ma, and J. Zhou, "Sustainable synthesis of apricot shell-derived hierarchical porous carbon for supercapacitors: A novel mild one-step synthesis process," Coll. and Surf. A: Physic.and Eng. Aspects, 637, 128257, 2022.
[7] T. S. Temirgaliyeva et al., "Self-supporting hybrid supercapacitor electrodes based on carbon nanotube and activated carbons," Eur. Chem.Techn. Jour., vol. 20, no. 3, pp. 169–175, 2018.
[8] H. Eom, J. Kim, I. Nam, and S. Bae, "Recycling black tea waste biomass as activated porous carbon for long life cycle supercapacitor electrodes," Mater., vol. 14, no. 21, 2021.
[9] E. Canbaz, "Findik Kabuklarindan Hidrotermal Karbonizasyon Yöntemi ile Karbon Malzemelerinin Eldesi Ve Sodyum-Iyon Bataryalar Için Kullanim Potansiyelinin Incelenmesi," Gebze Teknik Üni., 2020, (In Turkish).
[10] A. B. Fuertes et al., "Chemical and structural properties of carbonaceous products obtained by pyrolysis and hydrothermal carbonisation of corn stover," Soil Res., vol. 48, no. 7, pp. 618–626, Sep. 2010.

[11] K. Aydıncak, "Hidrotermal karbonizasyon yöntemiyle gerçek ve model biyokütlelerden karbon nanoküre sentezi ve karakterizasyonu," Ankara Üniversitesi, 2012, (In Turkish).
[12] S. Román, J. M. Valente Nabais, B. Ledesma, J. F. González, C. Laginhas, and M. M. Titirici, "Production of low-cost adsorbents with tunable surface chemistry by conjunction of hydrothermal carbonization and activation processes," Microp. and Mesop. Mater., vol. 165, pp. 127–133, Jan. 2013.
[13] K. Q. Tran, A. J. Klemsdal, W. Zhang, J. Sandquist, L. Wang, and Ø. Skreiberg, "Fast Hydrothermal Liquefaction of Native and Torrefied Wood," Ener. Proc., vol. 105, pp. 218–223, May 2017.
[14] B. K. Kızılduman, "Pirinç Kabuğundan Hidrotermal Karbonizasyon Yöntemi ile Karbon Küre Üretilmesi ve Enerji ve İlaç Salimi Alaninda Kullanilabilirliğinin Araştırılması," Balikesir Üniversitesi, 2020, (In Turkish).
[15] E. Unur, S. Brutti, S. Panero, and B. Scrosati, "Nanoporous carbons from hydrothermally treated biomass as anode materials for lithium ion batteries," Microp. and Mesop. Mater., vol. 174, pp. 25–33, Jul. 2013.
[16] M. Süner, "Hidrotermal Karbonizasyon Yöntemi ile Çay Tesis Atiklari ve Badem Kabuklarindan Aktif Karbon Üretimi," Firat Üniversitesi, 2022, (In Turkish).
[17] M. I. Satayev, R. S. Alibekov, L. M. Satayeva, O. P. Baiysbay, and B. Z. Mutaliyeva, "Characteristics of activated carbons prepared from apricot kernel shells by mechanical, chemical and thermal activations," Mod Appl Sci, vol. 9, no. 6, pp. 104–119, 2015.
[18] T. Wang, Y. Zhai, Y. Zhu, C. Li, and G. Zeng, "A review of the hydrothermal carbonization of biomass waste for hydrochar formation: Process conditions, fundamentals, and physicochemical properties," Renew. and Sustain. Ener. Rev., vol. 90, pp. 223–247, Jul. 2018.
[19] B. Janković et al., "Physico-chemical characterization of carbonized apricot kernel shell as precursor for activated carbon preparation in clean technology utilization," J Clean Prod, vol. 236, p. 117614, Nov. 2019.
[20] K. Aljoumaa, H. Tabeikh, and M. Abboudi, "Characterization of apricot kernel shells (Prunus armeniaca) by FTIR spectroscopy, DSC and TGA," Jour. of the Indian Acad. of Wood Sci., vol. 14, no. 2, pp. 127–132, Dec. 2017.
[21] J. Krumins, M. Klavins, and V. Seglins, "Comparative Study of Peat Composition by using FT-IR Spectroscopy," Mater. Sci. and Appl. Chem., vol. 26, p. 106, 2012.
[22] Y. Lin, X. Ma, X. Peng, and Z. Yu, "A mechanism study on hydrothermal carbonization of waste textile," Ener. and Fuels, vol. 30, no. 9, pp. 7746–7754, Sep. 2016.
[23] B. K. Via, O. Fasina, and H. Pan, "Assessment of pine biomass density through mid-infrared spectroscopy and multivariate modeling," Biores., vol. 6, no. 1, pp. 807–822, Apr. 2013.
[24] J. Jayaramudu, S. C. Agwuncha, S. S. Ray, E. R. Sadiku, and A. Varada Rajulu, "Studies on the chemical resistance and mechanical properties of natural polyalthia cerasoides woven fabric/glass hybridized epoxy composites," Adv Mater Lett, vol. 6, no. 2, pp. 114–119, Feb. 2015.
[25] S. Fong Sim, M. Mohamed, N. Aida Lu Mohd Irwan Lu, N. P. Safitri Sarman, and S. Nor Sihariddh Samsudin, "Computer-assisted analysis of Fourier Transform Infrared (FTIR) spectra for characterization of various treated and untreated agriculture biomass.," Bioresour., vol. 7, no. 4, pp. 5367–5380, 2012.
[26] N. A. Nikonenko, D. K. Buslov, N. I. Sushko, R. G. Zhbankov, and B. I. Stepanov, "Investigation of stretching vibrations of glycosidic linkages in disaccharides and polysaccarides with use of IR spectra deconvolution," Wiley Online LibraryNA Original Res. on Biomol., pp. 257–262, 2000.
[27] J. Cao, G. Xiao, X. Xu, D. Shen, and B. Jin, "Study on carbonization of lignin by TG-FTIR and high-temperature carbonization reactor," Fuel Proce. Techn. vol. 106, pp. 41–47, Feb. 2013.
[28] M. A. Islam, M. J. Ahmed, W. A. Khanday, M. Asif, and B. H. Hameed, "Mesoporous activated coconut shell-derived hydrochar prepared via hydrothermal carbonization-NaOH activation for methylene blue adsorption," J Env. Manage, vol. 203, pp. 237–244, Dec. 2017.
[29] G. Sivasankarapillai and A. G. McDonald, "Synthesis and properties of lignin-highly branched poly (ester-amine) polymeric systems," Bio. Bioen., vol. 35, no. 2, pp. 919–931, Feb. 2011.
[30] B. E. Obinaju and F. L. Martin, "ATR-FTIR spectroscopy reveals polycyclic aromatic hydrocarbon contamination despite relatively pristine site characteristics: Results of a field study in the Niger Delta," Environ Int, vol. 89–90, pp. 93–101, Apr. 2016.
[31] X. Zhao et al., "Efficient solid-phase synthesis of acetylated lignin and a comparison of the properties of different modified lignins," J Appl Polym Sci, vol. 134, no. 1, p. 44276, Jan. 2017.
[32] S. Başakçılardan Kabakcı and S. S. Baran, "Hydrothermal carbonization of various lignocellulosics: Fuel characteristics of hydrochars and surface characteristics of activated hydrochars," Waste Manag., vol. 100, pp. 259–268, Dec. 2019.
[33] Z. Liu, A. Quek, S. Kent Hoekman, and R. Balasubramanian, "Production of solid biochar fuel from waste biomass by hydrothermal carbonization," Fuel, vol. 103, pp. 943–949, Jan. 2013.